Characterization of acid solids by proton/deuterium exchange followed by infrared spectroscopy

Catarina Simão Marta[a,b*]

[a]*Instituto Superior Técnico, Avenida Rovisco Pais 1, 1049-001 Lisboa, Portugal*

[b]*IFP Energies nouvelles, Rond-point de l'échangeur de Solaize, BP 3, 69360 Solaize, France*

Abstract

The present report concerns the development of an infrared spectroscopy characterization technique capable of precisely describing the surface acidity of zeolites, whose surface properties comprehension is of key importance for their efficient application as catalysts.

This methodology is based on the use of perdeuterated benzene (C_6D_6) as a probe molecule, forming deuteroxyl groups (OD) at the expense of hydroxyl groups (OH) which behave as Brønsted acid sites, catalytically active. The H/D exchange is followed according to the increasing time contacts of the sample with C_6D_6.

Faujasite zeolites with different Si/Al ratios and subjected to different thermal treatments were used to validate this methodology. The results have shown that this technique is capable of simultaneously characterizing most of the acid sites found on zeolites, screening their accessibility and their acidic strength. Additionally, it is sensitive enough to study the influence of distinct parameters, such as the distribution of acid sites according to the Si/Al ratio, and the alteration of the acidity by modification treatments. The results were obtained on a wavenumber range which only contains the hydroxyl groups that have undergone H/D exchange, providing more detailed information on the distribution and quantification of the acid sites when compared to other probe molecules and characterization techniques.

Keywords: zeolite Y, H/D exchange, infrared, spectroscopy, characterization, perdeuterobenzene

1. Introduction

It is thanks to catalysis that a large number of reactions and industrial processes can be carried out at operating conditions that make them economically feasible, and there is no shortage of examples that illustrate its importance and contribution to currently employed industrial processes. For instance, the synthesis of ammonia by the Haber-Bosch process (1909) was the first process carried out on a large-scale, providing an extreme reduction of the severity of operating conditions needed to obtain this compound. Other processes worth mentioning are the Fischer-Tropsch process to convert synthesis gas to motor fuels (1923) and the catalytic cracking of oil (1936) [1].

Catalytic processes are carried out by employing catalysts. The introduction of a catalyst provides a new reaction pathway, more energetically favorable than the original route, as it reduces the energy of activation, accelerating the reaction. The most commonly employed are aluminosilicates such as zeolites, clays and amorphous silica alumina (ASA), but other types of acid solids can be applied as well, such as magnesium, zinc and cerium oxides, alumina, silica and metal organic frameworks (MOF), to name a few [2,3].

Zeolites are one of the most important classes of catalysts, extensively used in industry due to their molecular sieving, shape selectivity and ion exchanging properties [2]. These are very porous aluminosilicates, with a structure composed by submicroscopic interconnected channels [4].

They have a tridimensional structure formed by TO_4 tetrahedra (SiO_4 or AlO_4^- , as T=Si or Al atoms) linked together by oxygen atoms [2,5,6], which originate the unit cells, described by expression *(1)* [2], where n relates to the valence of the cation M, x and y are the total number of tetrahedra by unit cell and y/x is equivalent to the atomic Si/Al ratio.

$$M_{x/y}^{n+}(AlO_2^-)_x(SiO_2)_y \qquad (1)$$

Silicon tetrahedra are neutrally charged, as the positive charges in Si^{4+} are balanced by each of the oxygen anions to which it is bound. As a result of aluminum in its Al^{3+} ionic form, aluminum tetrahedra are negatively charged [3]. In order to achieve electroneutrality, these negative charges need to be balanced out by compensation cations, usually sodium (Na^+) or other alkaline or alkaline earth metals.

The compensation cation can be easily removed by ion exchange, during synthesis or post synthesis treatments and the most interesting is when these metal cations are replaced by protons, constituting Brønsted acid sites (BAS), responsible for the catalytic activity of zeolites [5]. Aside from BAS, zeolites can also contain Lewis acid sites (LAS), basic sites and redox centers, making them suitable for applications in acid, basic, acid-base, redox and bi-functional catalysis [2].

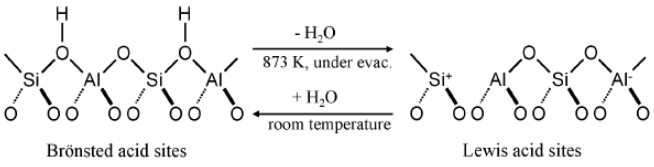

Figure 1: Brønsted and Lewis acid sites in catalysts [7]

Zeolites contain pores of molecular dimensions, ranging from 3–12 Å to 0.5–1.2 nm [5,8,9]. Depending on the dimensions and on the type of structure, they can display micro-, meso- or macroporosity, or a combination thereof. The porous framework can be defined as uni-, bi- or tridimensional, containing channels that may or may not be interconnected. The unique porous structure in each zeolite accounts for their shape selectivity and for the rates and modes of diffusion of different molecules. Preferential diffusion paths may exist depending on the relative sizes of the reactants and products [5]. Thus, these solids can act as molecular sieves, being able to separate different molecules according to their shape and dimensions.

Zeolites can be formed naturally in alkaline environments with volcanic activity (~40 known types), but most of the zeolites employed in industrial processes are artificially synthesized, with more than 200 types presently identified [10]. The first synthetically prepared zeolite was coined zeolite A and made from Na, Si, and Al by Linde [8]. Following zeolite A, zeolite X and Y were synthesized, and they are currently extensively used in catalytic cracking processes [8]. Both zeolites have a faujasite type structure, illustrated in Figure 2.

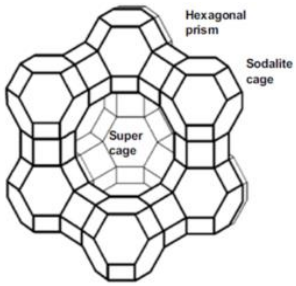

Figure 2 : Faujasite structure. Adapted from [10]

The serious stability constraints found on zeolite X led to its replacement by zeolite Y, more hydrothermally stable due to its lower acidity (containing only 50% of the total acidity found in X zeolite [11]), and its higher SiO_2/Al_2O_3 ratio (Si/Al = 2.5). Zeolite Y has a major advantage over its X counterpart, as its Si/Al ratio can be increased and tuned using steam and/or acid treatments, while largely maintaining the crystallinity.

Ultrastable Y (USY) zeolite appeared in the late 1970s and resulted from a framework dealuminated version of Y zeolite by calcination of its NH_4 form [12], followed by thermal treatment in the presence of steam under controlled temperatures.

Calcination directly influences several textural properties, such as the specific area, the porosity volume and the pore size distribution. Additionally, it can indirectly affect the activity, selectivity and stability of the catalyst. The main objective of this treatment is to create porosity while simultaneously increasing the mechanical strength of the catalyst [2]. Two different transformations can occur during calcination: one concerning the thermal decomposition of the active agents' precursors, the release of volatile substances and the formation of porosity, and the other related to the modification of the structure's crystalline/ amorphous profile.

Steaming is one of the many hydrothermal transformations that a catalyst can be subjected to, responsible for the stabilization of the structure and for making it more resistant to high temperatures [13,14]. By removing the aluminum content in the catalyst, the Si/Al ratio increases, and the overall acidity decreases. The dealumination of Y zeolites makes it possible to modulate the activity of the zeolite by controlling the Si/Al ratio of the framework and, therefore, the number of acid sites. The density of acid sites decreases upon dealumination, in turn affecting the porosity, polarity (hydrophobicity) and reactivity.

Steam stabilized catalysts, like USY, are industrially popular as they are less prone to surface modifications [13], avoiding structure collapse, for instance. The Si/Al ratio is usually kept around 6 or higher in these catalysts, resulting in improved catalytic and hydrothermal stability.

Presently, Y and USY zeolites are used in various petrochemical applications, due to their remarkable activity and (shape) selectivity. Among different applications, USY zeolites are used in hydrocracking processes aiming at the conversion of vacuum gas oil (VGO) to middle distillates, reducing the selectivity towards gasoline and gas and thus complying to the high diesel demands of the automobile industry [15].

The catalytic activity of aqueous solutions can be predicted by the Hammett function, H_0, which employs a visual acidity scale built by using colored indicators, i.e. weak bases that can be easily converted to their conjugate acid by stronger acids. In aqueous solutions, the acid density or acid strength are often used as synonyms, as the universal acid responsible for proton transfer to a base is the hydroxonium cation H_3O^+ [2] . Thus, the extent of protonation depends mostly on the concentration of these ions and not on the acid strength of the dissolved acid.

However, acid solids usually have an heterogenous surface, giving rise to a broad distribution of acid sites of distinct individual strength and density, like BAS coexisting and even interacting with LAS. Thus, this method is not capable of discerning the strengths of the acid sites found simultaneously on the surface of an acid solid, and often more than one characterization technique is needed to correlate the acidity to the catalytic activity of acid solids [16].

Adsorption-Desorption methods, namely adsorption microcalorimetry or temperature programmed desorption (TPD), are attractive as they are relatively cheap. Both can provide information on the acid amount, the acid strength and the distribution of acid sites, but the latter is run under more realistic operation conditions, providing more reliable information [16].

Microcalorimetry measures the heat exchanged during adsorption of a certain probe on a clean surface. It consists in keeping the zeolite sample at a constant temperature in a sealed microcalorimeter [16], while pulses of probe molecule (usually pyridine or ammonia) are introduced at increasing vapor pressure to titrate the acid sites from highest to lowest strength [17]. Nevertheless, this technique may not be easily correlated with others, which is a significant drawback.

Temperature-programmed desorption starts with the sample already saturated in probe molecule (most commonly ammonia, but pyridine, carbon monoxide or water can also be used) and is performed at a constant heating rate between an initial and a final temperature, following a temperature program [16,17]. The acquired heat flow curve gives information on the amount of desorbed species as a function of time, either by measuring the mass variation or by analyzing the outlet gas stream [17].

Nevertheless, this technique only provides significative results if the experimental conditions are strictly controlled. The interpretation of the results can be very complex, as the heat of adsorption can be affected by confinement effects, by the slow diffusion or the readsorption of probe molecules. Lastly, this technique is not capable of distinguishing between BAS and LAS [17].

Nuclear magnetic resonance (NMR) spectroscopy can be used to study the chemical composition, the structure or location of relevant T-atoms (framework vs. extra-framework species, surface vs. inner sites), balancing metals and protonic acid sites, and it can also be used for adsorption and diffusion studies [16,17].

Magic angle spinning (MAS) consists in rapidly spinning the sample around an axis forming a specific angle (the magic angle – 54,74°) with the direction of the external magnetic field, to minimize the effects of the immobility of the molecules and anisotropic interactions, as well as to cancel the effect of dipole-dipole interactions [16].

Different nuclei can be studied by MAS-NMR. For instance, ^{29}Si and ^{27}Al determine the concentration of the acid sites, whereas ^{17}O, ^{1}H, ^{15}N, and ^{31}P provide information on the acid strength of BAS [17]. Similar to IR, probe molecules can also be used, with the most common being pyridine, carbon monoxide or acetone. Bulkier probe molecules can be used, to distinguish between surface and inner acid sites.

However, this is a very costly technique, due to the probes and to the equipment that is used, and the preparation of the sample/rotor that should be done in a glovebox. Additionally, the low temperatures that are used are different from those employed in catalytic processes, providing misleading conclusions on the performance of the catalyst.

Model reactions offer a reliable alternative to characterize the strength and density of different acid sites, using analysis conditions closer to the real catalytic conditions [18]. Additionally, they allow the

distinction between BAS and LAS. Nevertheless, the acidity of zeolites can only be fully characterized by employing several different reactions, as only the sites reactive to a certain reaction will be characterized [17]. Other problems may be related to confinement effects, which affect the concentration of reactant molecules near the active sites and, consequently, the reaction rate.

Infrared spectroscopy has been crucial for collecting information about the acidic properties of catalysts, such as zeolites. This field was revolutionized with the Fourier Transform Infrared (FT-IR) spectrometers, which considerable decreased the time needed to obtain a spectrum in the whole range of frequencies, decreased the energy loss, and gave much higher signal to noise ratio [19].

The mid infrared region (4000-400 cm^{-1}) is the most studied, as this interval comprises the vibronic modes of typical groups, like zeolites hydroxyl groups (BAS) [16,17], and provides information on the distortion of the T-O bond length or of the T-O-T or O-T-O angles (by observing the bands appearing between 1000 and 850 cm^{-1}).

IR experiments are usually carried out in transmission mode, by measuring the transmittance, i.e. the ratio between the incident intensity read on the detector, I, and the incident intensity, I_o. The transmittance can also be given by equation *(2)*, where ε_ν is the molar absorption coefficient ($mol^{-1}\ dm^2\ cm^{-1}$) at a certain frequency ν and ce relates to the number of adsorbing species n (in mmol) per surface of the pellet (in cm^2), S, given by equation *(3)*.

$$T = \frac{I}{I_o} = e^{-\varepsilon_\nu ce} \qquad (2)$$

$$ce = \frac{n}{S} \qquad (3)$$

The transmittance can be easily converted to absorbance, d, by employing the Beer-Lambert equation *(4)*.

$$d = log_{10}\left(\frac{1}{T}\right) \qquad (4)$$

Stronger Brønsted sites (of higher acidity) can be found at lower wavenumbers [6,17]. A way of distinguishing between Brønsted sites in similar wavenumbers and of determining the presence of Lewis sites is by employing probe molecules. Lewis acid sites, LAS, are coordinatively unsaturated sites working as electron acceptors, and will bind to nucleophilic molecules. Brønsted acid sites, BAS, are proton donors, such as OH groups, and will form different complexes with basic molecules [6]. By following the adsorption, one can gather information on surface features, as well as the nature, strength, local arrangement and amount of different acids sites on the catalyst [16].

Some of the most commonly used probe molecules include pyridine, ammonia, carbon monoxide and benzene. Pyridine is a strong base that forms three complexes on the surface of an oxide (see Figure 3), which can be observed between 1400 cm^{-1} and 1700 cm^{-1}: PyH^+ (pyridinium ion), PyL (coordinated to Lewis acid sites) and Py-HO (hydrogen bonding). Its bigger dimensions may cause steric constraints, and difficulties in properly cleaning the setup after its introduction may also occur [16].

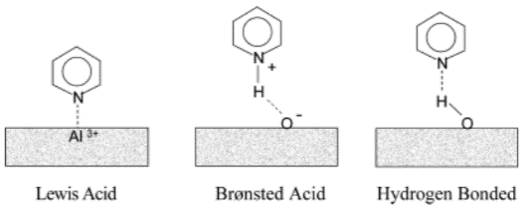

Figure 3 : Different pyridine complexes formed on a metal oxide surface [20]

Carbon monoxide is a small weak base that interacts with hydroxyl acid groups via H-bonding and with cationic acid sites [17]. As the interaction with the acid sites is weak, the adsorption must be performed at low temperatures (usually at 100 K using liquid nitrogen). The vibration bands for BAS can be found between 2138 and 2170 cm^{-1} and around 2240 cm^{-1} for LAS [6,16]. Some cons relate to difficulty in discerning between strong and weak acid sites, and its difficult quantification [1].

Ammonia is very popular due to its small dimensions, high stability and ability to distinguish between BAS and LAS. However, due to is very strong basicity, it can form numerous adsorbed species interacting with LAS, BAS and basic sites, showing poor selectivity [21].

Benzene is a weak base that interacts with protons via its π-electron cloud and can distinguish between acid sites with very close strength. However, the attribution to each of these sites might prove difficult and steric hindrances may also occur [6].

Deuterated benzene has been increasingly used to study zeolites and other acid solids [22]. By contacting with a deuterated probe molecule, the sample undergoes H/D exchange, i.e. the hydroxyl groups (OH) are exchanged by deuteroxyl groups (OD). As the deuteron is heavier than the proton, the signal is shifted to lower wavenumbers, the so called deuteroxyl region. The only contributions in this region are the OD species that have been created, thus the acid sites that have been exchanged. This does not occur in the hydroxyl region, which comprises contributions attributed to non-acidic groups in addition to acid sites. Thus, this probe molecule allows the distinction between acid sites of similar strength and their accurate quantification.

As such, the aim of this work was to characterize the acidity on a set of faujasite Y and USY zeolites, by employing infrared spectroscopy, and perdeuterobenzene (C_6D_6) as a probe molecule.

2. Experimental Part

2.1. Experimental Procedure

2.1.1. Preparation of the wafer

Approximately 20 mg of pure sample were pressed into a self-supporting wafer with a surface area of ~ 2 cm^2. The pressing pressure was kept at 2 ton during 30 seconds in a *Specac Atlas Autotouch 8T* presser. The wafer should be thin enough to remain transparent in the mid-IR region and to prevent noisy and non-quantitative results, and gently pressed, as the usage of higher pressures can damage the structure of the solid or hinder the gas diffusion and adsorption of probe molecules during analysis. Additionally, the wafer should have a homogenous thickness, as the collected signal can be altered due to modifications in optical path of the infrared beam when the wafer thickness is not constant.

2.1.2 Activation of the wafer

The self-supporting wafer was placed inside a transmission cell with KBr windows, where it was subjected to an activation step aiming at the removal of unwanted surface species such as physisorbed water. This was done by using a programmable oven.

The first step consisted of heating up the sample from room temperature up to 100°C and keeping it at this temperature for at least one hour. A ramp step would follow, to increase the temperature up to 450°C. This temperature was kept for a minimum duration of 10 hours. The last step was to decrease the temperature back to 100°C, which was kept until the beginning of the experiment to prevent readsorption of water. The activation procedure has been performed in dynamic conditions under secondary vacuum with pressures around 10^{-6} mbar inside the cell.

2.1.3 Contact with probe molecule

Infrared spectra with a range between 4000 and 400 cm^{-1} were recorded in transmission mode using a *ThermoFischer Scientific Nicolet iS50* FT-IR spectrometer, equipped with a KBr beamsplitter and a DTGS (Deuterated Tryglicine Sulfate) thermal detector. Each spectrum was recorded with a resolution of 4 cm^{-1}, accumulating 40 scans per spectrum. The experiments were carried out under vacuum (pressures in the order of 10^{-6} mbar).

A background spectrum was recorded after thermal activation. Prior to contact with C_6D_6, an initial spectrum of the activated sample was also obtained. The sample was then put in contact with the probe molecule at room temperature, at first for 30 seconds. Contact times of 5 minutes and 10 minutes followed (with contacts of 20 minutes and 30 minutes for some of the samples). An evacuation step of approximately 15 minutes under dynamic secondary vacuum (pressure below 10^{-6} mbar) followed every contact in order to remove the excess C_6D_6 inside the setup, with a spectrum being recorded at the end of each of these steps. Note that the evacuation time for CBV500 and its calcined form required approximately 1 hour.

Some samples were heated up to 150°C after performing the contacts at room temperature. In this case, the contact with the probe molecule was done by successive periods with a fixed duration of 15 minutes, followed by 15 minutes evacuation, until the cumulative time of contact reached one hour at this temperature. Analogous with the procedure at room temperature, a spectrum was recorded at the end of each evacuation step.

3. Fourier Self Deconvolution (FSD)

Results obtained by infrared spectroscopy are usually deconvoluted, in order to distinguish between the different acid sites that are contributing to the resulting spectrum (overlapping contributions), and as a mean to obtain their relative quantification by integrating the area below each deconvoluted curve.

Deconvolution was the first tested methodology to develop a data treatment that could be reproducible and applicable to all the studied samples. However, the changing position of the bands due to the different characteristics in each type of tested zeolite gave non-comparable quantitative results between distinct samples. Additionally, deconvolution proved to be a very onerous task as the Si/Al ratio increased.

Direct area integration was posteriorly applied. For this technique, a baseline is chosen between the wavenumbers of interest. By using it as reference, the area concerning a specific range of wavenumbers comprised in the baseline can be directly taken, thus its terminology. Nevertheless, the tilting of the spectra was still not corrected.

Hence, all the spectra have been treated using Fourier Self-Deconvolution (FSD), a method that has been developed since the 1980s as a computer processing of spectral data, specifically of proteins [5]. It uses Fourier transforms and is comparable to first-order derivatives, allowing to study intrinsically overlapped band contours [23]. This method enhances the visualization of individual IR bands and suppresses baselines difficulties, but it does not improve the resolution. Furthermore, it cannot resolve an IR band into a single component unless this individual component was already in the original spectrum.

The quality of the collected information depends on two parameters, the line bandwidth (BW) and the enhancement factor (EF), defined, respectively, as the width of the spectral line at half-height and the ratio of line bandwidth before and after deconvolution. Additionally, the signal to noise ratio of the original spectrum should be appropriately high to enable the resolution of the spectrum into individual components [5], without enhancing the noise. Optimal values for these parameters were determined to be an EF of 1,5 and a BW of 20 cm^{-1} for the studied zeolitic samples.

The advantages of this treatment are especially clear in the deuteroxyl region (see Figure 4). The treated spectrum shows more defined and pronounced bands for the different acid sites. Nevertheless, the effect of FSD is less pronounced on samples with lower Si/Al ratio, as the expression of the overlapped bands is not as intense.

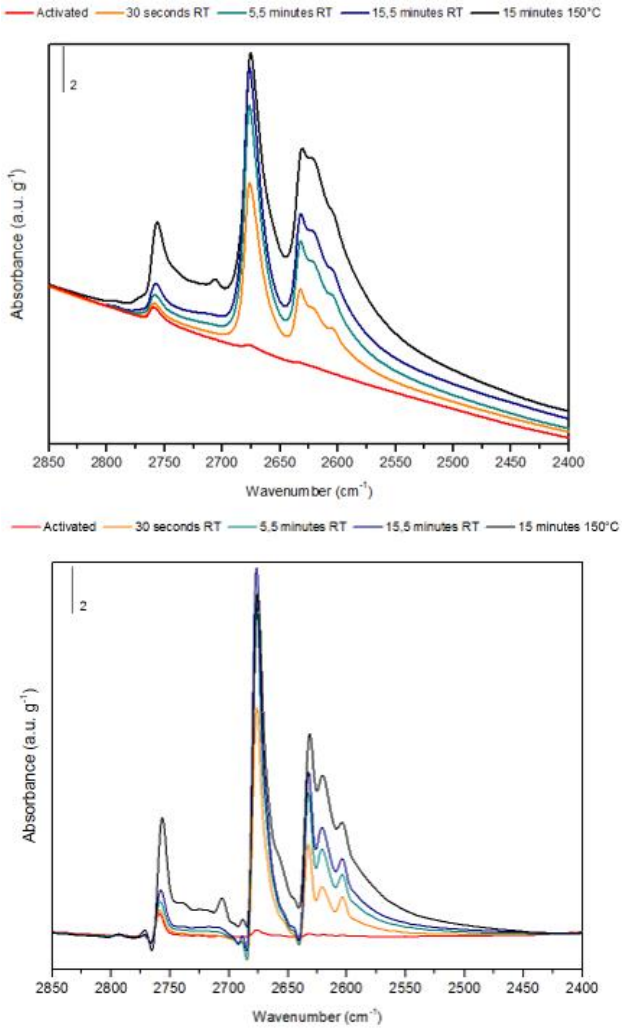

Figure 4 : Spectra comparison in the deuteroxyl region of CBV720 before (top) and after (bottom) Fourier Self Deconvolution

One of the biggest advantages when employing this treatment is the correction of the baseline. As all spectra are treated in the same manner, the quantification of the acid sites can be easily performed by direct integration, not only for spectra concerning different exchange times on the same sample, but when comparing different types of samples as well.

4. Results and Discussion

4.1. Description of the samples

Commercial faujasite zeolites provided by *Zeolyst* and without any posterior modification were characterized (see Table 1), ranging from CBV500, a purely microporous Y zeolite in its ammonia form, to CBV760, a mesoporous zeolite in its protonated form.

The effect of calcination was studied on CBV500 and CBV712, as well as the effects of conventional steaming and acid treatment in liquid phase on CBV720 were also studied. Finally, the shaping effect

was also studied, with both commercial CBV720 and the sample modified by acid treatment have being mixed with an alumina binder.

Table 1 : Overview of commercial faujasite zeolites from *Zeolyst*. Adapted from [11]

CBV code	SiO_2/Al_2O_3 Mole Ratio	Si/Al (mol mol^{-1})	Cation	NaO_2 Weight %	Unit cell size (Å)	Surface Area ($m^2\ g^{-1}$)
500	5,2	2.6	NH_4^+	0,2	24,53	750
712	12	6	NH_4^+	0,05	24,35	730
720	30	15	H^+	0,03	24,28	780
760	60	30	H^+	0,03	24,24	720

4.2. Band Attribution

The band attribution employed in the hydroxyl region can be consulted in Table 2 and in Figure 5, using CBV720 as example.

Table 2 : Band attribution of different acid sites in zeolites for the hydroxyl region

Hydroxyl type	Definition	v(OH) (cm^{-1})
External SiOH	SiOHext	3745
Internal SiOH (Perturbation Si(OH)…Al)	SiOHint	3736
Partially extra-framework AlOH	AlOH	3670
Supercage framework Si(OH)Al	HFOH	3629
Sodalite cage framework Si(OH)Al	LFOH	3564
Perturbed Si(OH)Al by extra-framework Al	HF'OH	3602
	LF''OH	3550
	LF'OH	3525

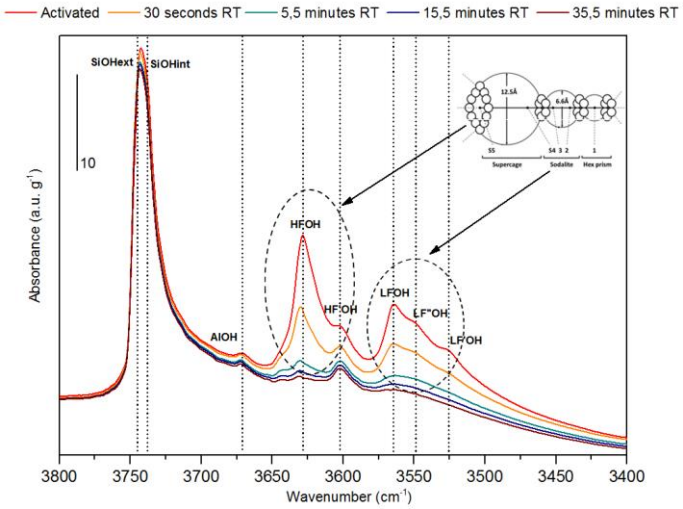

Figure 5 : Band attribution for the hydroxyl region of CBV720. Different spectra after contact with C_6D_6 are represented

As the H/D exchange unfolds, the signal previously seen in the hydroxyl region is shifted to lower wavenumbers (the deuteroxyl region) due to the heavier mass of deuterium compared to the proton. The ratio between the wavenumbers of the bands in the hydroxyl and the deuteroxyl region is of ~1,35.

Once more using CBV720 as example, the bands attribution observed in the deuteroxyl region can be consulted in Table 3 and Figure 6.

Table 3 : Band attribution of different acid sites in zeolites for the deuteroxyl region

Deuteroxyl type	Definition	v(OD) (cm^{-1})
External SiOD	SiODext	2762
Internal SiOD (Perturbation Si(OD)…Al)	SiODint	2755
Partially extra-framework AlOD	AlOD	2706
Supercage framework Si(OD)Al	HFOD	2676
Sodalite cage framework Si(OD)Al	LFOD	2628
Perturbed Si(OD)Al by extra-framework Al	HF'OD	2656
	LF''OD	2618
	LF'OD	2599

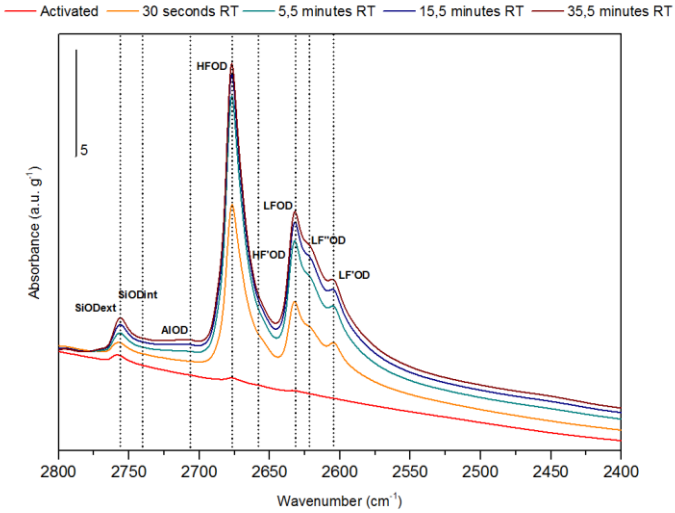

Figure 6 : Band attribution for the deuteroxyl region of CBV720. Different spectra after contact with C_6D_6 are represented

4.3. Effect of the Si/Al ratio

The activated spectrum of CBV500 (see top of Figure 7) shows striking differences from the rest, possibly due to the presence of NaOH species, and a higher concentration of aluminols due to extraframework species at 3670 cm^{-1}. Additionally, a much weaker silanol signal can be reported on CBV500, in line with its lowest Si/Al ratio and low mesoporosity.

This sample displays the highest concentration of stronger acid sites, i.e. HF'OH and LF'OH sites in the deuteroxyl region (see bottom of Figure 7), after 15 minutes exchange. However, it seems that a larger distribution of strong acid sites is present, opposed to very defined bands related to LF'' and LF' (at 2618 cm^{-1} and 2600 cm^{-1} respectively) observed on both CBV712 and CBV720.

It would be expected to see the almost total exchange of perturbed acid sites (HF'OH, LF''OH and LF'OH) after 15 minutes contact with C_6D_6, as these portray higher acidity, but a considerable portion of these sites has not undergone exchange, and the ratio of total exchanged sites is lower than the ones for HFOH and LFOH. These

results may be a consequence of a better accessibility for these latter groups, thus exchanging faster, despite the lower acid strength. In fact, this hypothesis is reasonable in the case of LF''OH and LF'OH, the perturbed sites in the sodalite cage, as the H/D exchange occurs by secondary means such as proton/deuteron migration between LF and HF groups, and possibly due to an established equilibrium between (HF)OH/(LF)OH distribution and hopping of a proton from one oxygen site to another in the same aluminum-occupied oxygen tetrahedron [1]. Still, as the exchange occurs by direct contact in the supercage, why HF undergoes exchange at a higher rate than HF' remains unanswered.

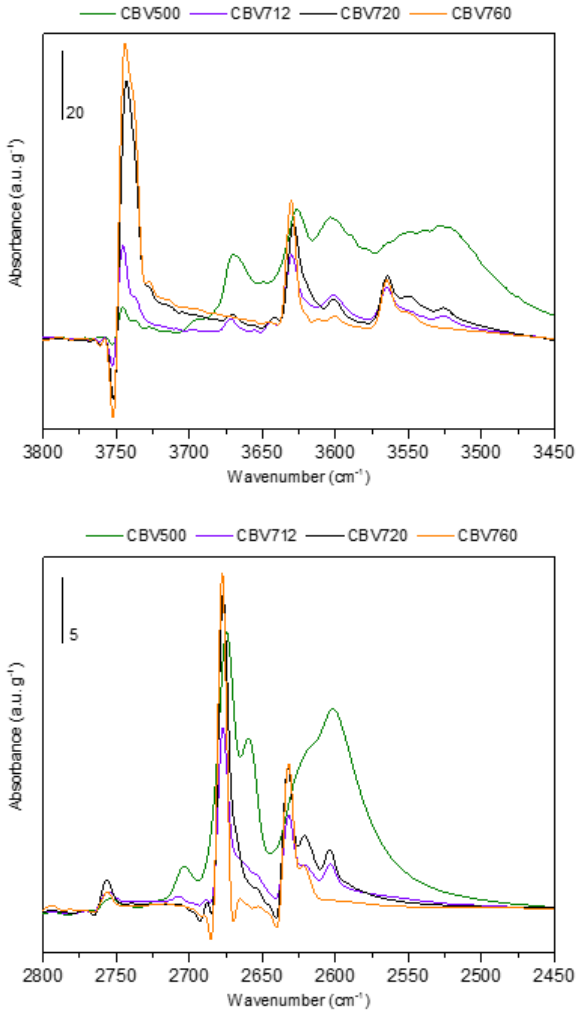

Figure 7 : Si/Al effect on different faujasite zeolites. Activated spectra (top) in the hydroxyl region and spectra after 15 minutes contact with C_6D_6 in the deuteroxyl region (bottom)

CBV760 appears to be the less acidic zeolite (in line with its highest Si/Al ratio), due to the overall less intense bands, namely the almost imperceptible shoulder for HF' and LF'', and the lacking LF' band on both the hydroxyl and the deuteroxyl spectra. A part of these enhanced sites appears to be gained back as LF and LF groups, when comparing the thinner and more intense bands with the analogous bands collected for CBV712 and CBV720. The highest silanol band in this sample is a result of its higher mesoporosity and high Si/Al ratio. Nevertheless, it seems that the acid sites found in this sample undergo almost full H/D exchange after 15 minutes contact, a result of its open mesoporous structure. This leads to the conclusions that the acid sites found on CBV760 are more accessible and/ or stronger than in others, which might result from the treatments it was subjected to.

The decrease of acidity when going from CBV712 to CBV720 creates a sharper and more intense band for HF acid sites, at the expense of the perturbed HF' sites of higher acidity. This can also be pointed out for the very pronounced increase of intensity reported for the silanol contribution found in CBV720. Notwithstanding, CBV720 appears to bear more perturbed low frequency acid sites (LF'' and LF' bands) than CBV712, in theory the most acidic of the two.This may be due to the acid leaching performed on this sample which, despite increasing the Si/Al ratio, keeps the framework ratio, thus creating a more mesoporous sample which possibly allows quicker H/D exchange.

The total acidic OH (HF, HF', LF,LF' and LF'') available to be exchanged on the activated spectra shows a different trend from the total OD created that has been created after 15 minutes exchange (Figure 8, A and B). The former decreases with the increasing Si/Al ratio, in line with the decrease of aluminum. The latter decreases from CBV500 to CBV712 but, afterwards, it increases as the Si/Al increases. Thus, dealumination may not affect all acid sites in the same manner when the Si/ Al increases, with the strong acid sites being kept intact. When calculating the ratio between the total OD formed after 15 minutes at room temperature and the total acidic OH available in the activated spectra, there is an increase in the proportion of stronger acid sites prone to exchange at room temperature as Si/Al increases (Figure 8, C). So, despite the samples having less acidity, the remaining acid sites have stronger acidity, resulting in a higher proportion of OD being created.

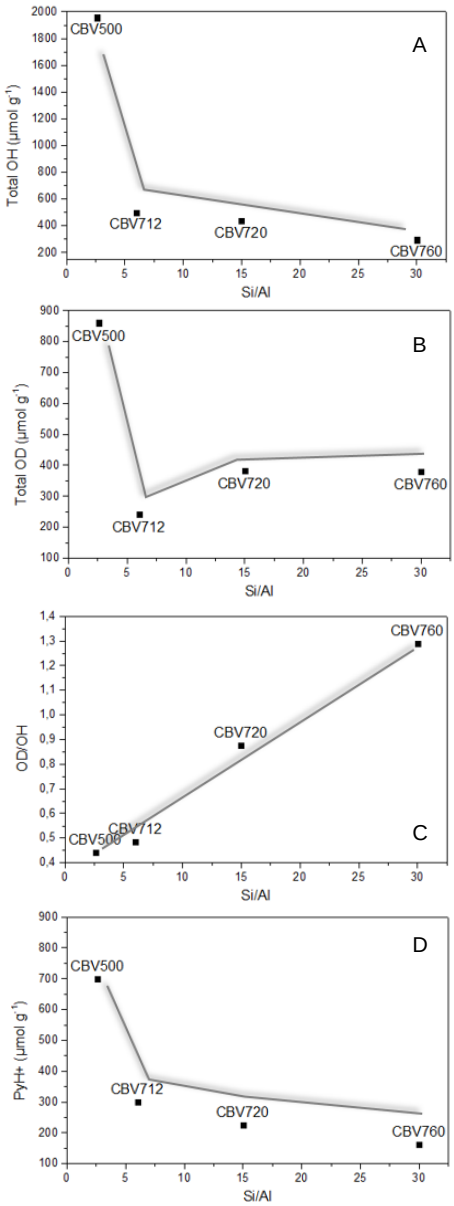

Figure 8 : Results according to the Si/Al ratio: A-concentration of total acidic OH on the activated spectra, B- total concentration of OD exchanged after 15 minutes contact at room temperature, C- ratio

between OD created and total OH available, D- pyridinium concentration

The results obtained when using pyridine (Figure 8, D) are concomitant with those obtained for the total acidic OH, but not with the total OD formed after 15 minutes contact at room temperature. This may be due to the first contact being performed at 150ºC, providing information on all the acid sites that can be exchanged at this temperature. When using C_6D_6, the exchange starts at room temperature so the first information to be acquired is related to the concentration of strong acid sites.

4.4. Calcination Effect

The effect of calcination has been studied for two different types of NH_4 form Y and USY zeolites, CBV500 and CBV712. A loss of acidity can be reported on both samples upon calcination when observing the activated spectra, especially for CBV500, as a great part of the intensity of the bands concerning HF and LF is lost (see Figure 9). Additionally, calcination appears to have created a different site distribution, observed in the higher intensity of the HF' sites and on the much lower LF' shoulder. Furthermore, an increase of the silanol groups occurs when calcination is performed, resulting from the loss of part of the micropores and in the destruction of part of the acid sites, especially the acid sites in the LF and LF' range, which are those found in the sodalite cages.

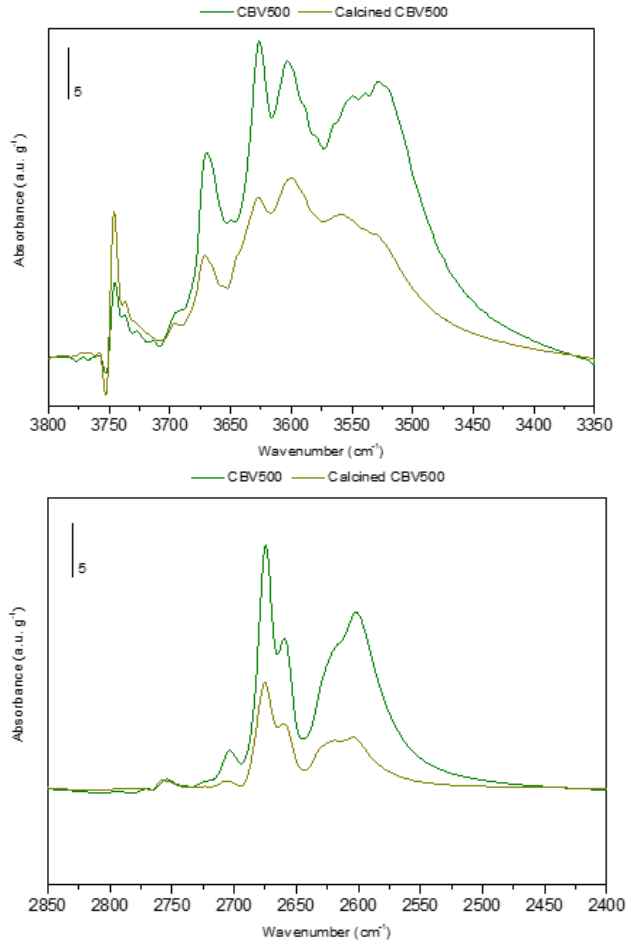

Figure 9 : Calcination effect on CBV500. Activated spectra (top) in the hydroxyl region and spectra after 15 minutes contact on the deuteroxyl region (bottom)

The overall loss of acidity on CBV712 upon calcination is not as extreme, but it seems to have affected all acid sites in the same proportion when looking at the activated spectra (top of Figure 9). The calcined form of CBV712 shows a lower intensity of the extra-framework aluminum band (3670 cm^{-1}). When looking at the deuteroxyl region of the spectra for the CBV712 samples, there isn't much of a loss on the HF and LF groups, which leads to believe that the sites lost upon calcination are not exchangeable at room temperature (i.e. weak acid sites). The exact opposite happens for the perturbed HF' and LF' sites. In fact, the behavior found for the most acid sites is similar, but a very pronounced HF' shoulder comprising two different contributions, can be found on the calcined sample (bottom of Figure 9), different from the sloped contribution found on CBV712.

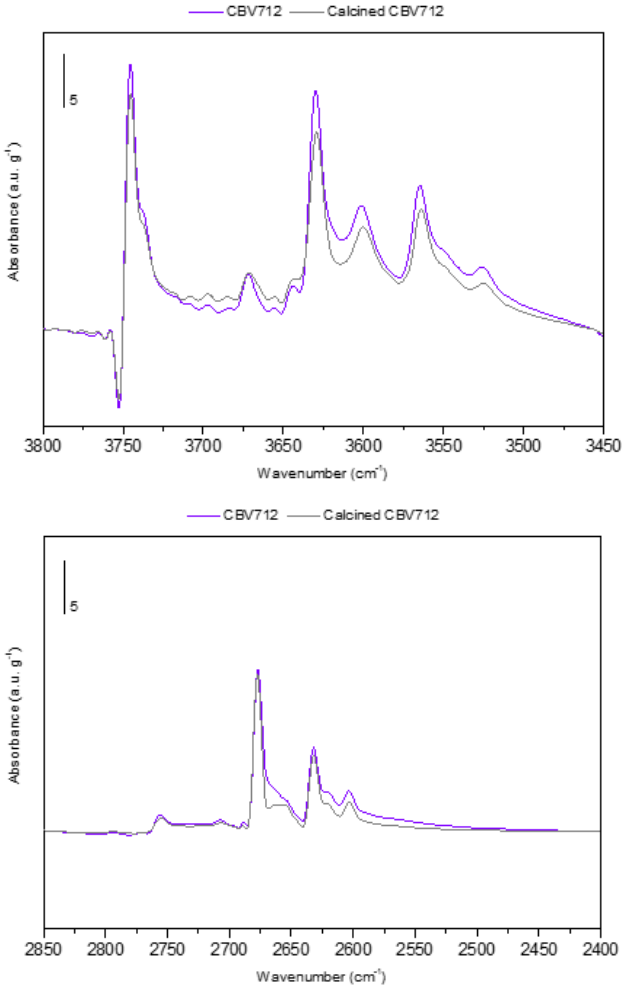

Figure 10 : Calcination effect on CBV712. Activated spectra (top) in the hydroxyl region and spectra after 15 minutes contact on the deuteroxyl region (bottom)

When comparing the OD/OH results for these samples, the calcined CBV500 shows a lower value than its parent zeolite (0,32 compared to 0,44), whereas the calcined CBV712 shows a higher value (0,55 opposed to 0,49) Concerning the first case, these results may be a consequence of pore blocking, or to accessibility or diffusional constraints on calcined CBV500 due to its purely microporous structure. As for CBV712, the ratio increases due to the loss of some of its weak acid sites.

4.5. Modification Effect

CBV720 has been subjected to modification by two different procedures: conventional steaming (Steamed CBV720) and by acid treatment in liquid phase (Modified CBV720).

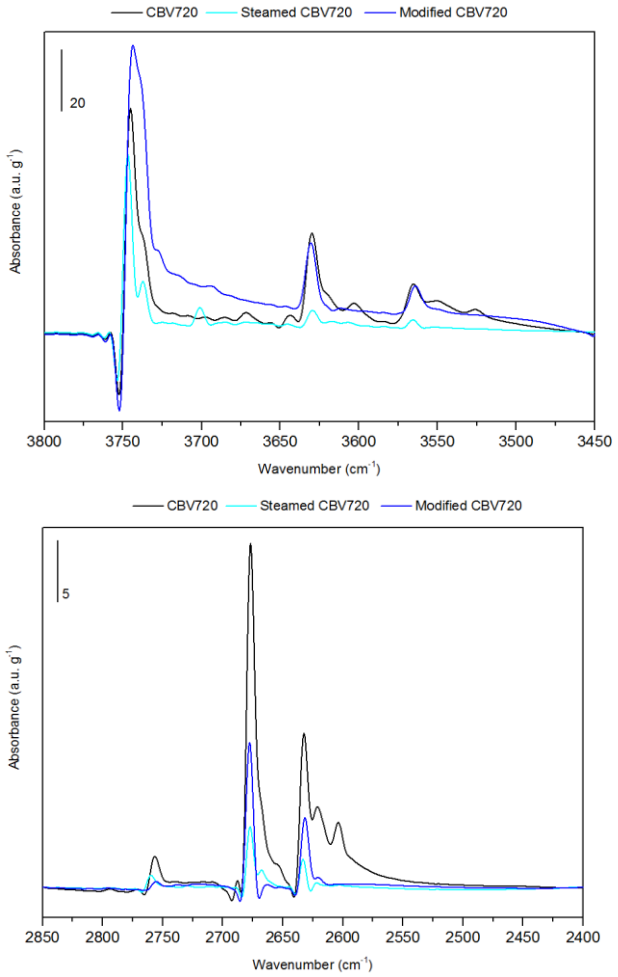

Figure 11 : Modified CBV720 by steaming or by acid treatment. Comparison between activated spectra (top) and spectra after 15 minutes contact for the deuteroxyl region (bottom)

Most of the original acidity is removed when the parent zeolite is steamed. Just by looking at the activated spectra (see top of Figure 11), one can easily spot the absence of the very defined bands seen on the parent sample attributed to the high frequency and the low frequency acid sites. Specifically, the bands related to perturbed species are almost imperceptible in the resulting steamed spectra, whereas the HF and LF signal are present, but with a much lower intensity. Additionally, there appears to be a new contribution at 3700 cm^{-1} that cannot be spotted in the parent zeolite. This new component could be assigned to OH oligomeric Al species. Lastly, even though there is a shoulder at 3738 cm^{-1} on the original sample, the ensuing steamed sample shows a much more defined shoulder at the same wavenumber, even if its overall intensity is lower.

When looking at the deuteroxyl region (see bottom of Figure 11), almost all the available acid sites on both the steamed and the parent zeolite have undergone H/D exchange after 15 minutes contact, except for the silanol groups (weakly acidic) and the new contribution created on the steamed sample (otherwise the corresponding band at ~2740 cm^{-1} should be present in the spectra). As such, the oligomeric Al species should portray a very weakly or non-acidic behavior. Furthermore, a very short contribution of perturbed HF' acid sites can be observed in the deuteroxyl region for the steamed sample, not discerned in the hydroxyl spectra.

A very broad contribution between 3730 cm^{-1} and 3460 cm^{-1} can be found on the Modified CBV720. The short band found in the deuteroxyl spectra at 2620 cm^{-1} can be attributed to LF'OH sites. The presence of this band could not be envisioned when looking at the hydroxyl spectra, masked by the broad effect of the bands in this region. Despite the intensity of the HFOH and the LFOH bands being somewhat kept after acid treatment, a part of these sites does not exchange after 15 minutes, whereas an extended level of exchange can be seen for the parent zeolite. In fact, the HFOD and LFOD bands on the modified sample show around half of the intensity of the corresponding bands on CBV720.

Furthermore, when calculating the OD/OH ratio, the steamed sample shows a much higher value (~1) than what is obtained for the modified sample and for the parent zeolite (respectively, 0,45 and 0,88), translating into a higher proportion of strong acid sites that can easily undergo exchange.

This is mainly due to the fact that acid treatment forms silanol nests, seen by the noticeable band on the quantitative results concerning the silanol sites and by the broad band found on the spectra for the corresponding wavenumbers. The dealumination is possibly more selective towards the sites of enhanced acidity than what is obtained by steaming, where the removal of the overall acidity is much more extensive and not just limited to groups of enhanced acidity.

4.6. Shaping Effect

Both the parent CBV720 zeolite and its modified version by acid treatment were mixed with an alumina binder.

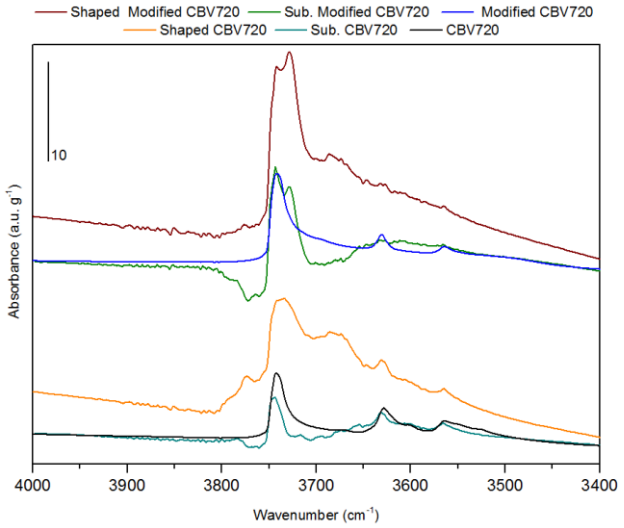

Figure 12 : Shaping effect on CBV720. Comparison between activated spectra of CBV720 and modified CBV720 before and after shaping in the hydroxyl region. The spectrum resulting from the subtraction of the alumina binder to the shaped zeolites are also included for both cases

Striking differences in the aspect of the activated spectra (see Figure 12) can be distinguished after shaping, mostly due to the contribution of the alumina binder. When subtracting the contribution of the alumina binder to the spectra of the modified samples, one should obtain their zeolite content. The subtracted and the original spectra are not superposable, concluding that the shaping step induces modifications on the zeolite (despite the zeolite content being the same, when comparing the bands at ~1800cm^{-1}, concerning the T-O-T vibration modes of the zeolite). There is a different distribution of the acid sites, with part of the aluminols being consumed (as seen by the negative signal found at ~3768 cm^{-1} and 3720 cm^{-1}), as well as a small fraction of the HFOH, and all contributions on the LF region. It seems, as well, that the bands for LF''OH and LF'OH are no longer distinguishable.

As for the activated spectrum for the shaped modified sample, its profile is closer to what would be obtained for a non-shaped zeolite, apart from the new band that can be observed at ~3730 cm^{-1}, not found on the non-modified shaped zeolite.

By comparison between the subtracted and the original spectra of the modified zeolite, an even more pronounced consumption of the aluminols can be reported. However, differently from what found on the parent zeolite, the bands attributed to both the HFOH and LFOH groups are difficult to visualize and replaced by a broad band at ~3650 cm^{-1}. The most interesting feature falls on the new band at 3730 cm^{-1}, thus concluding that shaping of the modified sample created a new OH species and a distinct distribution of the acid sites. The extent of the shaping induced alterations is much more prominent on this sample than on the shaped non modified CBV720.

This new contribution is clearly exchanged after 15 minutes at room temperature, evidenced in the OD region at ~2750cm^{-1} (see Figure 13). Additionally, it is one of the first species to undergo exchange and reach an equilibrium, proving to display an acidity close to that of hydroxyl acid sites.

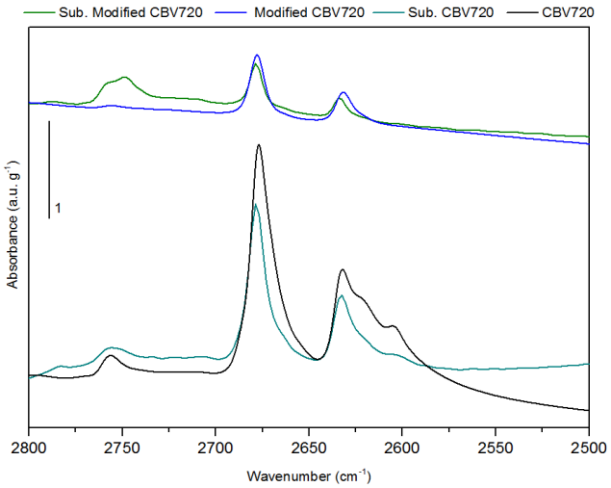

Figure 13 : Shaping effect on CBV720. Comparison between spectra of CBV720 and modified CBV720 before and after shaping after 15 minutes exchange at room temperature in the deuteroxyl region. The spectrum resulting from the subtraction of the alumina binder to the shaped zeolites are also included for both cases

5. Conclusions and Future works

Different characterization techniques have been developed to study the acid sites of zeolites and other catalysts, but these are often incapable of discriminating and/or quantifying between each type of acid sites, only providing an estimation of the bulk acidity.

In line with the obtained results, employing C_6D_6 as a probe molecule can be used to simultaneously characterize most of the acid sites found on zeolites. It also allows to follow the H/D exchange as a function of the exchange time for all different types of sites, screening their accessibility and their acidic strength. Additionally, it proves to be sensitive enough to study the influence of distinct parameters on the acidity, such as the distribution of acid sites according to the Si/Al ratio, and the effects of modification treatments, namely calcination, steaming or acid treatment or, even, the effect induced by the shaping step.

Nevertheless, the shaping effect should be studied in further detail in order to determine the nature and origin of the new contribution found on the shaped modified CBV720.

More future works of interest would be to test this methodology with other types of probe molecules. In fact, a bulkier molecule, deuterated trimethylbenzene (1,3,5-Trimethylbenzene-d_{12}, *Sigma Aldrich*, 98 atom % D), has been tested in the present study for CBV500, CBV720 and the modified CBV720. By studying these samples, it was aimed to determine how the exchange could be affected by spatial and diffusional constraints, namely concerning the microporous profile of CBV500.

The experimental procedure had to be modified when using this probe molecule, as the removal of the physisorbed species inside the setup would not occur at room temperature, regardless of the duration of the evacuation step. Due to this, the first contacts at room temperature were performed in the same manner as previously addressed for C_6D_6, but the first information on the exchange was obtained only after evacuation at 150ºC. As the temperature was increased, a dual effect might have been at play: the evacuation of the physisorbed species and the enhancement of the exchange by less acidic sites.

Considering the above, only the results obtained after 30 minutes exchange at higher temperature have been compared to the equivalent results when using C_6D_6. Additionally, instead of the introduction of 20 mbar of probe molecule in each contact, a fixed value of 3 mbar has been used, due to the impossibility of increasing the vapor pressure to higher values when using deuterated trimethylbenzene. The comparison between the obtained results for each probe molecule can be seen in Figure 14.

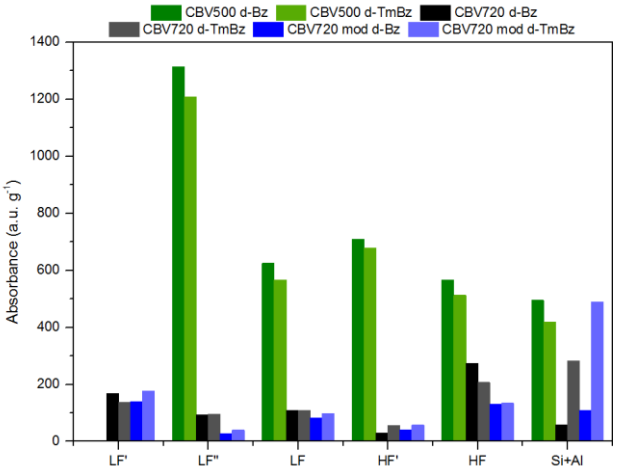

Figure 14 : Quantification of acid sites on CBV500, CBV720 and modified CBV720 in the deuteroxyl region, when using deuterated benzene (d-Bz) and deuterated trimethylbenzene (d-TmBz) as probe molecule

Not many differences can be found between the amount of acid sites probed by C_6D_6 and by deuterated trimethylbenzene. An increase in the exchange of the enhanced HF' sites can be discerned for CBV720 and its modified version when using this bulkier molecule, as well as LF, LF'' and LF' on the modified CBV720. Thus, the accessibility of the acid sites remains the same, regardless of the probe molecule that was used. The most striking differences are found for CBV500, where the quantification of the acid sites is lower when using deuterated trimethylbenzene instead of C_6D_6, possibly due to its microporous structure.

A future work of interest would be to test an even bulkier molecule, such as triisopropylbenzene. However, the deuterated molecule is not available, so the experimental procedure would have to be modified. One way would be to perform full H/D exchange using C_6D_6, and then make the sample contact with triisopropylbenzene, in order to follow the D/H exchange, obtaining information on the accessibility of the sites.

Another possibility would be to test different experimental procedures for the same probe molecule. Perhaps, the most interesting would be to increase the temperature for a fixed contact time, opposite of the experimental procedure employed in the present report. This way, one would be studying the acid strength and availability of the sites (as the increase in temperature will enable the

diffusion of the probe molecule, and the contact with more confined acid sites). Information on the temperature at which the total H/D exchange is reached would also be obtained.

The effect of the vapor pressure should also be investigated, as this parameter regulates the amount of gas phase C_6D_6 introduced in the setup. This way, it would be possible to determine, for instance, when saturation of the sites is reached. An experiment on CBV720 where 3 mbar of C_6D_6 has been introduced in each contact was also performed. The comparison between the results collected in this case and when using 20 mbar is found in Figure 15.

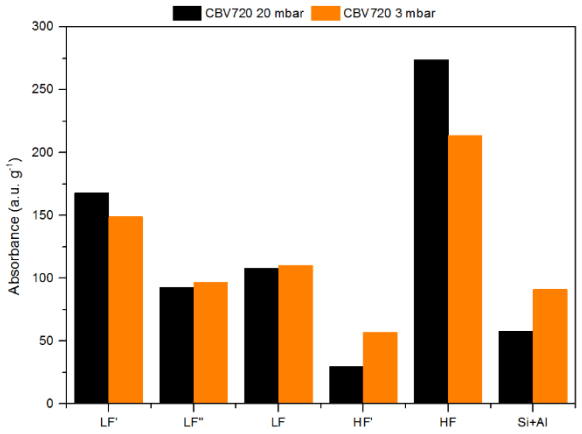

Figure 15 : Quantification of acid sites on CBV720, using a vapor pressure of 20 mbar and 3 mbar

It appears that the extent of exchange when using 20 mbar and 3 mbar is similar. However, further studies are necessary in order to validate the significance of these results.

6. References

[1] Poduval D. G. *On the role of acidity in amorphous silica-alumina based catalysts*. Technische Universiteit Eindhoven, 2011, 177 p.

[2] Figueiredo J. L., Ribeiro F. R., Lemos F., Orfão J. J. M. *Catálise heterogénea*. Fundação Calouste Gulbenkian, Lisboa, 2015, 352 p.

[3] Hadjiivanov K. *Identification and Characterization of Surface Hydroxyl Groups by Infrared Spectroscopy*. Elsevier, 2014, 220 p.

[4] Speight J. G. *The Refinery of the Future*. Elsevier Science, 2010.

[5] Vazhnova T., Lukyanov D.B. Fourier self-deconvolution of the IR spectra as a tool for investigation of distinct functional groups in porous materials : Brønsted acid sites in zeolites, *Analytical chemistry*, 2013, 85, 23, 11291-11296. DOI: 10.1021/ac4020337.

[6] Che M., Vedrine J. C. *Characterization of solid materials and heterogeneous catalysts : From structure to surface reactivity*. Wiley-VCH, Weinheim, 2012, 48 p.

[7] Kondo J.N., Nishitani R., Yoda E., Yokoi T., Tatsumi T., Domen K. A comparative IR characterization of acidic sites on HY zeolite by pyridine and CO probes with silica-alumina and γ-alumina references, *Physical chemistry chemical physics : PCCP*, 2010, 12, 37, 11576-11586. DOI: 10.1039/c0cp00203h.

[8] Chester A.W. Zeolite Characterization and Catalysis: A Tutorial, Springer 2009, 373 p.

[9] F. R. Ribeiro, J. L. Figueiredo. *Catálise Heterogénea*. Fundação Calouste Gulbenkian, Lisboa, Portugal, 2015.

[10] Karge H. G., Weitkamp J., Baerlocher C., Bennett J. M., Depmeier W., Fitch A. N., Jobic H., van Koningsveld H., Meier W. M., Pfenninger A., Terasaki O. *Structures and Structure Determination*. Springer Berlin Heidelberg, Berlin, Heidelberg, 1999.

[11] Verboekend D., Nuttens N., Locus R., van Aelst J., Verolme P., Groen J.C., Pérez-Ramírez J., Sels B.F. Synthesis, characterisation, and catalytic evaluation of hierarchical faujasite zeolites : Milestones, challenges, and future directions, *Chemical Society reviews*, 2016, 45, 12, 3331-3352. DOI: 10.1039/c5cs00520e.

[12] Jacobs P. U.J.B. Infrared study of deep-bed calcined NH_4Y zeolites, *Journal of Catalysis*, 1971, 22, 2, 193-203. DOI: 10.1016/0021-9517(71)90185-0.

[13] Scherzer J., Bass Jonathan L. Infrared spectra of ultrastable zeolites derived from type Y zeolites, *Journal of Catalysis*, 1973, 28, 1, 101-115. DOI: 10.1016/0021-9517(73)90184-X.

[14] Cairon O. Impacts of composition and post-treatment on the Bronsted acidity of steam-treated faujasite : Insights from FTIR spectroscopy, *Chemphyschem : a European journal of chemical physics and physical chemistry*, 2013, 14, 1, 244-251. DOI: 10.1002/cphc.201200568.

[15] Dufresne P., Bigeard P.H., Billon A. New developments in hydrocracking : Low pressure high-conversion hydrocracking, *Catalysis Today*, 1987, 1, 4, 367-384. DOI: 10.1016/0920-5861(87)80005-6.

[16] Sandoval-Díaz L.E., González-Amaya J.A, Trujillo C.A. General aspects of zeolite acidity characterization, *Microporous and Mesoporous Materials*, 2015, 215, 229-243. DOI: 10.1016/j.micromeso.2015.04.038.

[17] Derouane E.G., Védrine J.C., Pinto R.R., Borges P.M., Costa L., Lemos M.A.N.D.A., Lemos F., Ribeiro F.R. The Acidity of Zeolites : Concepts, Measurements and Relation to Catalysis: A Review on Experimental and Theoretical Methods for the Study of Zeolite Acidity, *Catalysis Reviews*, 2013, 55, 4, 454-515. DOI: 10.1080/01614940.2013.822266.

[18] Kotrel S., Lunsford J.H., Knözinger H. Characterizing Zeolite Acidity by Spectroscopic and Catalytic Means : A Comparison, *The Journal of Physical Chemistry B*, 2001, 105, 18, 3917-3921. DOI: 10.1021/jp002161v.

[19] Karge H.G., Geidel E. Vibrational Spectroscopy, in *Molecular sieves* : *Science and technology.* Éd. H. G. Karge, J. Weitkamp. Springer-Verlag, Berlin, New York, 1998-, 1-200.

[20] Layman K.A., Ivey M.M., Hemminger J.C. Pyridine Adsorption and Acid/Base Complex Formation on Ultrathin Films of γ-Al_2O_3 on NiAl(100), *The Journal of Physical Chemistry B*, 2003, 107, 33, 8538-8546. DOI: 10.1021/jp030046p.

[21] Bourne K.H., Cannings F.R., Pitkethly R.C. Structure and properties of acid sites in a mixed-oxide system. I. Synthesis and infrared characterization, *The Journal of Physical Chemistry*, 1970, 74, 10, 2197-2205. DOI: 10.1021/j100909a028.

[22] Hensen E.J.M., Poduval D.G., Degirmenci V., Ligthart D.A.J. M., Chen W., Maugé F., Rigutto M.S., van Veen J.R. Acidity Characterization of Amorphous Silica–Alumina, *The Journal of Physical Chemistry C*, 2012, 116, 40, 21416-21429. DOI: 10.1021/jp309182f.

[23] Kauppinen J.K., Moffatt D.J., Mantsch H.H., Cameron D.G. Fourier transforms in the computation of self-deconvoluted and first-order derivative spectra of overlapped band contours, Analytical Chemistry, 1981, 53, 9, 1454-1457. DOI: 10.1021/ac00232a034.